Design Techniques for Thermal Management in Switch Mode Converters

Erik C. W. de Jong, *Student Member, IEEE*, J. A. Ferreira, *Fellow, IEEE*, and Pavol Bauer, *Member, IEEE*

Abstract—Thermal management plays a pivotal role in achieving high power densities in converters. Improvement on thermal performance of critical components in printed-circuit board (PCB) assembled switch mode converters is achieved by using design techniques that extend across electromagnetic, geometrical, and thermal-integration technologies. For better use of the already available PCB material, three-dimensional component layout and flexible PCB technology are utilized to gain advantages. A theory to evaluate the thermal-management effectiveness of switch mode converters is introduced based on two new figures of merit, namely thermal-management loss density and thermal-design rating. These two figures of merit quantify the effective use of thermal-management material as well as the thermal performance of a converter design. The figure-of-merit criteria allow flexibility so that it can be adjusted to an appropriate design objective. Design objectives include achieving higher power densities or achieving good reliability. The thermal-management-effectiveness theory is applied here to thermally optimize a Flyback converter that has been geometrically integrated. The design technique to adjust the thermal-management effectiveness of integrated switch mode converters to achieve a set objective, by means of the introduced figures of merit, forms the core of the publication, validated by experimental measurements.

Index Terms—AC–DC power conversion, design methodology, finite-difference methods (FDMs), optimization methods, printed-circuit board (PCB) assembled power supplies, thermal management, thermal variables control.

I. INTRODUCTION

THERMAL management plays a predominant role in the extent to which switch mode converters can be miniaturized. The increased loss density associated with increasing power density needs to be managed properly if the reliability and ultimately product lifetime of the miniaturized converter is to be upheld or even improved upon [1]. To increase the power densities by improving material usage, a design technique is required that provides a good interaction between the integration technologies implemented toward converter miniaturization and the thermal management thereof [2]. Integration technologies using planar technology [3], [4] and embedded functionality [5], [6] result in low-profile converters with large

top and bottom surfaces. This particular aspect ratio is advantageous for thermal management by natural cooling [7]. Planar designs do not necessarily lead to high power densities, especially if the converter requires energy-storage capacity or needs to process power directly from the grid. Therefore, integration technologies using three-dimensional (3-D) packaging principles have been developed [8]–[10], which result in volumetrically dense structures but is associated with high localized temperatures created by the increased difficulty of heat extraction from components, which are now deeply embedded in the converter structure. A combination of these integration technologies could therefore lead to increased power densities in the smallest nonplanar volume. Fig. 1 illustrates this combination of the two integration technologies by showing the components that benefit from integration by using 3-D packaging principles [energy-storage and low-frequency components located on top of the printed-circuit board (PCB)] and those that benefit from integration technologies leading to low-profile converters (passive components eligible for electromagnetic integration into the PCB itself). Furthermore, overall thermal integration is then responsible for achieving meaningful improvements in power density and simultaneously maintaining reliability. The conceptual integration processes will be highlighted next.

A. Geometrical Integration

The minimum volume that a component can occupy is determined directly by the function it needs to fulfil. A practical limit therefore exists for the low-frequency and energy-storage components in a converter that prohibits any further volume reductions of the physical component dimensions below a certain minimum. Further improvement on power density of such components should then be sought in the layout and packaging of the component packages using geometrical integration. The geometrical-integration process can be considered as a 3-D puzzle with the low-frequency components as irregular-shaped puzzle pieces. The aim of this challenge is then to thermally couple all the components, with the aid of various thermal interface materials, enclosing as little air as possible inside the converter system itself in the process. This allows for conductive heat sharing among components and is advantageous for achieving a uniform temperature distribution throughout the converter. Choosing complementary packages for components, i.e., packages that fit together well geometrically, eases the integration. Furthermore, exposing component surfaces that could aid in thermal transport adds more value to the already invested material. A good example of this is by exposing the metal
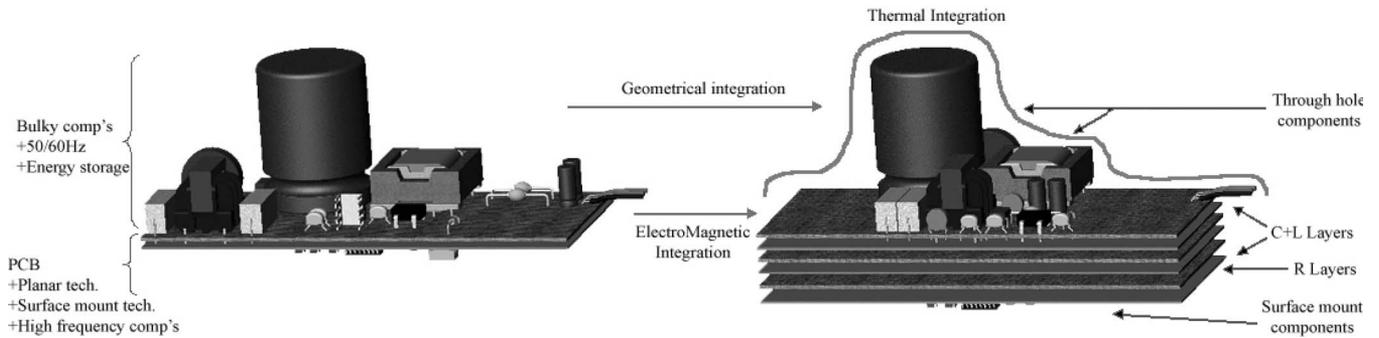
Fig. 1. Conceptual integration process in switch mode converters from (left) discrete component design to (right) more integrated design shown as semi-exploded view. Intercomponent thermal connection material is not shown for clarity.

canister of the usually large smoothing capacitor (electrolytic) to act as heat spreader for the converter system. Geometrical integration using a flexible substrate material for electrical interconnection has been shown to result in power-density improvements in dc–dc converters by Lostetter *et al.* [9].

B. Thermal Integration

The increase in loss density, due to the applied integration process(es), necessitates sturdy thermal management to sustain acceptable operating temperatures for the overall system as well as the individual components themselves. Integrated components, albeit geometrical or electromagnetic, experience a much greater thermal influence from neighboring components due to their close proximity. By implementing a structured thermal layout scheme, this can be exploited to tune individual component temperatures as well as establish a uniform thermal profile on the converter extremes. Operating components that show a strong relation between operating temperature and power dissipation at the materials' optimal temperature lead to enhanced electrical performance by lowered dissipation, as is the case for magnetic cores, for example. Furthermore, a uniform thermal profile establishes the largest temperature drop from converter to ambient, and from the generalized thermodynamic relationship of heat transport $q \approx \Delta T^x$, the heat flow rate increases with large ΔT, allowing for a higher tolerance of loss density. In order to assess improvements in switch mode converters' thermal management brought about by these integration methods among others, figures of merit are invaluable. First, they quantify the effective use of material used in a thermal-management function in order to optimize all available volume in a converter, and, second, they quantify how well the thermal management achieves its goal of keeping all individual components, not only at a safe but also at an optimal operating temperature [11], [12]. Optimal temperatures can be defined differently for set objectives such as reliability or high power density. Such figures of merit, which can ultimately be used to guide thermal designs from an early stage in a very specific objective-orientated manner or plainly be used to compare existing thermal-management techniques, are addressed in this paper to quantify advances brought about by the integration methods discussed. Moreover, this paper:

1) introduces two figures of merit to quantify thermal-management effectiveness in Section II;

2) applies the derived figures of merit as optimization technique for integration technologies on a case-study design consisting of two realizations of a Flyback converter in Sections III and IV;

3) performs validation as well as evaluation measurements on two synthesized Flyback converters, comparing power density and reliability objectives with the aid of the derived figures of merit in Section V.

II. THERMAL-MANAGEMENT EFFECTIVENESS

In most electrical designs, one strives to achieve the most functionality with little material and few parts. When doing thermal management in power electronics, the same principle can be applied. The thermal-management system should be as simple as possible, should not use many parts, and should use as little material as possible. To quantify the use of parts and material for thermal management and their subsequent thermal performance, two figures of merit are introduced. These are labeled thermal-management loss density (TMLD) and thermal-design rating (TDR). The first addresses the effectiveness of the implemented material and parts used for thermal management by volume, and the second addresses the thermal performance of the implemented material and parts. These two figures of merit are developed further in Sections II-A and II-B, respectively.

A. TMLD

Material intended for thermal management needs physical volume to transport heat. This necessity is a tradeoff between effective thermal transport and the adverse effects of thermal stressing on the material itself. Effective heat transport determines the effectiveness of the thermal management, and the level of thermal stressing of the material determines the lifetime and reliability of the overall thermal system. TMLD quantifies the effective use of implemented material and parts that perform a thermal-management function. It assesses the level of thermal loading of material and subsequently comments on the level of power density attainable in electronic assemblies. It is defined as the ratio between the electrical losses that need to be removed from a system and the volume of the thermal-management material that needs to transport the heat caused by these losses. TMLD is given by

$$\text{TMLD} = \frac{P_{\text{losses}}}{V_{\text{TM}}} \tag{1}$$

TABLE I
TMLD VALUES FOR COMMERCIALLY AVAILABLE POWER MOSFET PACKAGES EVALUATED FOR 1.2 W OF POWER DISSIPATION

		$SO-8$	$D-Pak$	D^2-Pak	$SOT-223$	$TO-220$	$TO-220I$	$TO-247$	$TO-273$
V_{tab}	$[mm^3]$	0.0	**16.8**	141.0	1.6	**199.0**	0.0	546.0	111.0
V_{pins}	$[mm^3]$	0.776	**3.490**	5.960	1.180	**12.240**	30.120	24.480	11.220
V_{TM}	$[mm^3]$	0.776	**20.320**	147.100	2.780	**211.180**	30.120	570.480	121.720
$TMLD$	$[W/cm^3]$	1546.4	**59.0**	8.1	431.6	**5.7**	39.8	2.1	9.8

and measured in watts per cubic meter. P_{losses} represents the total power dissipation. V_{TM} represents the volume of all the material contributing toward the thermal management of the converter.

Material volumes that contribute toward thermal management typically include the following.

1) Silicon die in semiconductor devices.
2) Electrically conductive paths. These include material for wire bonds, electrical package pins and tabs, package enclosures, and any additional wiring.
3) Cooling bodies and heat spreaders.
4) Thermal cladding, thermal potting material, and thermal interface material.
5) Interwinding isolation material in inductor and transformer structures.
6) Dedicated thermal layers on PCBs.
7) PCB tracks and any enclosure(s) attached to the PCB structure that assist in thermal transport.
8) Capacitor housings or any material that transports heat in a system.

1) Example—TMLD: To illustrate the TMLD approach, the Flyback MOSFET of the case study, presented in Section III, is considered here in a few commercially available packages. The volume for thermal-management material has been limited to only electrical conductive parts of the component, in this case, the electrical pins and package back plate for simplicity. For this MOSFET, packaged in a TO-220 package, the volume for thermal-management material consists of the package nonisolated back plate, or tab, and three electrical pins. This volume, calculated from geometries supplied in manufacturers' datasheets, occupies 211.18 mm^3 in total. Furthermore, it has a 1.2-W calculated power dissipation at rated power. By (1), the TMLD is then

$$\text{TMLD}_{(\text{TO-220})} = \frac{1.2}{211.18} \approx 5.7 \text{ W/cm}^3. \qquad (2)$$

The TMLD of the TO-220 package is shown alongside similar commercially available MOSFET packages in Table I. In the table, the volume of thermal-management material V_{TM} is the sum of the volume of the conductive back plate, or tab V_{tab} and the volume of the electrical pins V_{pins}. The comparison presented in Table I has been expanded across a wide range of packages to illustrate the diverse possibilities and how the TMLD value determines optimal packages for certain design objectives, in this case, power density. In practice, the choice of packages for a single component is usually limited to only two or three package types for this particular MOSFET to the

TO-220 and D-Pak types. Table I shows that if a MOSFET that meets all the electrical requirements for its chosen topology generates 1.2 W of losses, and it is available in all the packages shown, then from this comparison, the package with the highest TMLD value is most suited to achieve high power density when implemented in a converter. In this example, this is the small outline (SO-8) package with a very high TMLD value of 1546.4 W/cm^3. Seeing that the case-study MOSFET is only available in the TO-220 and D-Pak package, the choice is clear to change from the TO-220 package with a low TMLD value of 5.7 W/cm^3 in the discrete component design to the D-Pak with a TMLD value of 59 W/cm^3 in the more integrated-design converter. Attention should also be given to the operating surface temperatures of the respective packages by checking the thermal resistance of these packages. This is not explicitly shown in this example. Thus, by choosing this package, with high TMLD value as motivation to achieve a possible power-density objective, the thermal behavior of the electronic converter surrounding this component still needs to be considered for this prediction to become valid. A means to do this exactly is developed in Section II-B. For single components, the TMLD value might seem to be common sense for an experienced user; its real power lies when evaluating complete converter systems, where intuition might fall short.

B. TDR

The heat generated inside the components of an electronic converter results in temperature rise of the component material as well as that of the surrounding components. Due to the properties of the materials, they exhibit maximum and optimal operation temperatures. The optimal operation temperature of a component is a compromise between the lifetime, or reliability, of the component and the level of electromagnetic excitation of the component. Low operating temperatures; improve reliability; whereas, higher temperatures offer more efficient material usage due to a higher electromagnetic excitation capability. Furthermore, the convection rate of heat to the ambient from any component surface relies heavily on the difference between surface and ambient temperatures. A uniform temperature distribution on the component surface will therefore result in more effective convection of heat to the ambient due to a higher average temperature difference between surface and ambient allowing for a higher convection rate. This then results in overall lower component surface temperatures. Based on these statements, thermal management of an electronic converter must not only keep individual component material temperatures
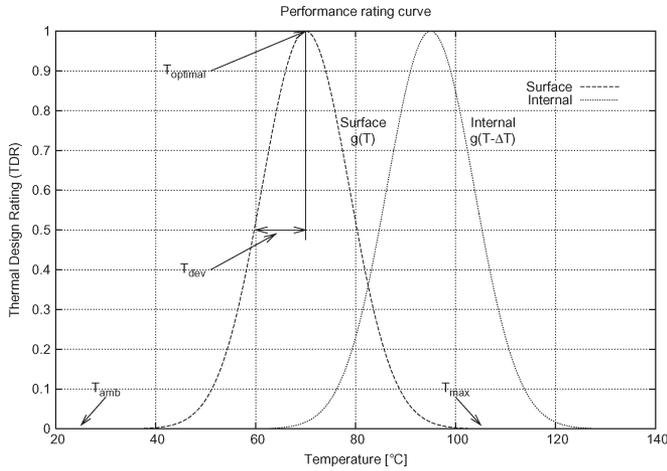
Fig. 2. Performance curve on which component temperatures are rated with component specific temperatures specified.

below their maximum but strive to keep the individual component material operating at its optimal operating temperature as well as create a uniformly distributed temperature profile on the convecting surface of the entire converter. If optimizing power density is an objective in converter design, then the thermal management, by means of material choice, operating temperature, and layout of components, can greatly improve on power density as components that share the same optimal operating temperatures can be placed very close together.

The TDR quantifies the thermal performance of a component, or system, as a result of its applied thermal management.

The rating is performed by means of a modified version of the statistical normal distribution curve given by

$$\text{TDR} \equiv g(T) = e^{-\frac{1}{2}\frac{(T - T_{\text{optimal}})^2}{2T_{\text{dev}}^2}} \tag{3}$$

where

$$T_{\text{dev}} = \frac{(T_{\text{max}} - T_{\text{optimal}})}{4} \qquad (T_{\text{dev}} > 0). \tag{4}$$

Determining the component specific temperatures T_{max} and, especially, T_{optimal}, is not an easy task. One might find maximum material temperatures in manufacturers' data sheets of components, or more generally, in physics textbooks. Finding the optimal temperature for a material or component requires either empirical data, good communication between designer and manufacturer of the respective components or should be based on component lifetime, and reliability constraints set by the designer. Fig. 2 shows the rating curve and the definitive temperatures used in (3) for achieving higher power density in converters rather than prolonged reliability. A similar curve can be constructed for optimization of reliability. The curve shape has been chosen for its rapid decay around its optimal point T_{optimal}, creating a sharp divide between temperatures close to and further away from the respective optimal material temperature. A rating between zero and one is assigned, where one represents thermal optimal performance and lower values lower performance and underutilization of implemented thermal material. Every type of component has its own ther-

mal rating curve; the main power-electronic types include the following:

1) power semiconductor;
2) different types of capacitors;
3) transformers with special core materials;
4) resistors.

The precision of the rating method is determined by the amount of individual rating curves defined and the accuracy of the component specific temperatures specified in the curves. The component internal hotspot temperature can also be rated and derived from surface temperatures, if component data are available for the power loss as well as thermal resistance between the surface and the internal hot spot. The thermal-path information is lumped into the temperature-drop term ΔT given by

$$\Delta T = R_\theta P_{\text{losses}} \tag{5}$$

where R_θ represents the thermal resistance from internal hotspot to the surface of the component. By adding (5) as a parameter to (3), the internal temperature rating curve $g(T - \Delta T)$ results. Fig. 2 shows both curves for internal and surface temperatures.

TDR of Systems: Until now, the TDR was developed based on ratings of single components in a converter. The single-component concept is developed further to include complete converter systems here. Two methods are proposed to determine a figure of merit for an overall converter. A weighted average of the individual component temperatures (surface or internal) can be evaluated, with the weights adjusted to emphasize the role of crucial components given by

$$\text{TDR}_{\text{ws}} = \frac{a_1 g(T_1) + a_2 g(T_2) + \cdots + a_n g(T_n)}{n}, \quad (0 \le a \le 1). \tag{6}$$

The motivation for choosing a certain weighing function relies on the objective of the evaluation. One could, for example, have similar weights for common components: all capacitors together, all ferrites together, and all resistors grouped together. A second option to evaluate TDR of systems is to calculate the ratio of how many components operate in a predefined optimal-temperature band, which is defined as having a thermal performance rating of α or higher against the total amount of components that are considered as

$$\text{TDR}_{\text{band}} = \frac{n \mapsto (g(T) < \alpha)}{n} \tag{7}$$

where the $n \mapsto$ (argument) operator counts the number of elements for which the argument, in this case temperature rating in optimal band, is true. A converter with all the power components operating at exactly its optimal value will have a TDR_{ws} and TDR_{band} of one, which is the asymptotic ideal value. An example of the TDR method is shown in [11] and will further be exemplified in the case study that follows. The case study will incorporate the technologies discussed until now and use the derived figure-of-merit system as design guideline.

TABLE II
COMPONENT PARAMETERS USED IN PERFORMANCE RATING CURVES
AND THERMAL-DESIGN EVALUATION ($T_{\mathrm{amb}} = 25\ ^{\circ}C$)

	$T_{optimal}[^{\circ}C]$		$T_{max}[^{\circ}C]$
	Power density	Reliability	
Capacitors	70	50	105
Magnetic cores	75	55	130
Silicon devices	110	75	150
Resistors	55	35	80

III. CASE STUDY

A case study illustrating the integration approaches discussed in Section I and the thermal-management figures of merit illustrated in Section II is performed on an isolated 20 W Flyback topology, similar to the case study of different converters performed in [11]. To determine the figure of merit for thermal effectiveness, the components need to be grouped in categories, each with their own set of maximum and optimum temperature values, according to Section II-B. The categories and their respective parameter values, for achieving high power density and achieving prolonged reliability of converters, used in this case study are given in Table II. It remains the designers' prerogative to design for reliability (converter lifetime), with its associated lower operating temperatures and lower achievable power density, or alternatively for high power density, knowingly sacrificing converter lifetime to obtain a small converter that operates very "hot." The TDR system caters for both.

The discrete converter with conventional thermal design will now be discussed in more detail, followed by two integrated-design solutions based on the integration methods of Section I.

A. Conventional Design

The design of the state-of-the-art ac–dc converter is governed by the direction in which power flows. The layout of components follows this pattern very closely as can be seen in Fig. 3(a), starting with the ac input on the left and working its way through the converter to the two output ports on the right. Single-sided PCB (FR4) is used with all through-hole components except for the control and control auxiliaries, which are implemented with surface-mount components on the bottom layer. The converters' thermal performance can be seen from the IR thermography results at full-load steady-state operation in Fig. 4(a). From these thermal images, all surface temperatures are extracted, and a thermal profile is created, as shown in Fig. 5(a). The figures of merit for the overall converter design is shown in Table V. These temperatures and figures of merit for thermal-management effectiveness dictate the thermal design and layout of the geometrically integrated converter solutions that will be discussed next.

B. Rigid-Flex Solution

Rigid-flex technology consists of nonflexible PCB material interlaced with flexible PCB material to allow the PCB to take on complex shapes but still exhibit mechanical strength and rigidity. A geometrically integrated solution using rigid-flex

technology is proposed in the form of a foldable converter, as shown in Fig. 3(b). The flexible PCB material, having a polyimide-based substrate, creates the hinges between the rigid PCB made from FR4 substrate. This allows for tight 3-D component placement and the possibility for electromagnetic integration in the rigid PCB segments. The TMLD value achieved by implementing this rather complex manufacturing process is shown in Table V.

C. Flex Solution

If it is not crucial for the PCB to provide mechanical support, then a geometrically integrated solution can be realized using only flexible PCB material. This solution is shown in Fig. 3(c). All components are laid out on a strip of flexible PCB material and then rolled up so that the edges of the PCB can be connected to the sides of the large electrolytic-capacitor canister. The components are then densely packed, utilizing all three available dimensions. Intercomponent space is optimized further by introducing thermal cladding and thermal grease to tightly couple the components thermally with each other for optimal heat sharing. The actual component placement is performed based on the design objectives set in Section I under the guidance of the figure-of-merit theory applied to the conventional design. The actual components are kept the same except for minor changes from through-hole technology to surface-mount technology to ease the electrical connectivity challenge of mainly the output rectifying components. This has been done to keep the respective component losses the same for both cases to be able to compare the influence of the geometrical integration and tight thermal coupling in a more isolated way. Once the influence is fully understood, then the individual component packages and material can be addressed. The TMLD values obtained for the fully flexible solution are shown in Table V. The design technique using figures of merit to guide the integration and thermal-management process will be the topic of discussion in the next section.

IV. DESIGN TECHNIQUE USING FIGURES OF MERIT

The temperature distribution profile of the conventional converter forms the basis for the geometrical- and thermal-integration process and directly influences the layout of the optimized converter. The design technique involves two steps: 1) identifying the required temperature change to have each component operate at its ideal temperature by making use of the thermal figures of merit and 2) creating a thermal profile from the component dissipation and geometrical information by using finite-difference analysis to act as thermal road map in locating suitable new locations for the components based on the figures of merit identified in the first step. The respective steps are discussed.

A. Thermal Figure-of-Merit Design Criteria

The measured surface temperatures of each component can be related to a thermal performance rating by following the procedure outlined in Section II and [11]. For the main power components, these ratings are shown in Table III. An adjustment
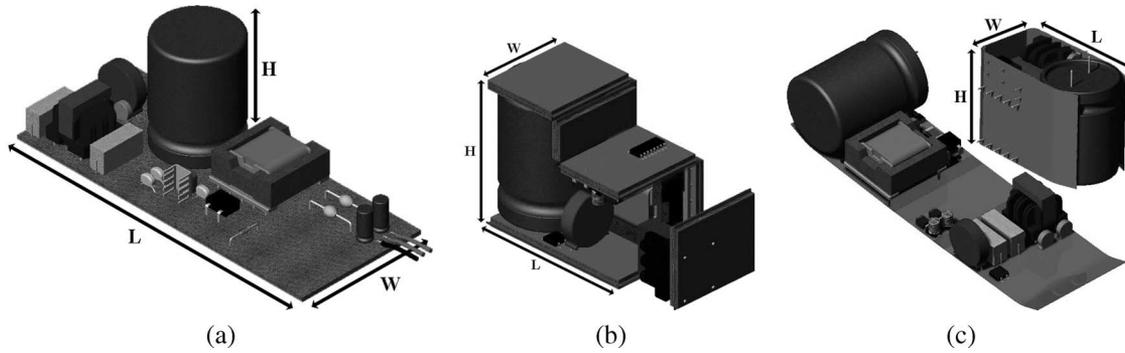
Fig. 3. Concepts of 20 W Flyback ac–dc converter illustrating power-density increase by means of geometrical and thermal integration. (a) Conventional thermal design and layout ($L \times W \times H = 118 \times 48 \times 44$ mm; power density $\approx 150\ W/l$). (b) Rigid-flex solution: Side panel removed and front panel exploded to show internal layout ($L \times W \times H = 60 \times 36 \times 46$ mm; power density $\approx 250\ W/l$). (c) Flex solution: Unrolled converter to show internal layout alongside final closed converter ($L \times W \times H = 58 \times 31 \times 37$ mm; power density $\approx 300\ W/l$).

temperature ΔT is calculated for each component, which indicates what temperature increase, or decrease, is necessary for each component to operate at its thermal optimum temperature. Furthermore, overheated components are identified as components that operate above their set optimal temperature, like the output diodes in the thermal image shown in Fig. 4(a), by a negative adjustment value, and on the other side, underheated components are components that operate under their optimal temperature, like the large electrolytic capacitor in the same image, by a positive adjustment value. The component-layout strategy is then based on the figure-of-merit criteria derived in Table III aided by the thermal profile generated by means of the mentioned finite-difference method (FDM).

B. Component Layout Strategy

Using the overheated component temperatures, a coarse thermal profile of the converter can be constructed using an FDM algorithm in any spreadsheet program, or if the converter has been built a thermal profile can be extracted from the thermal measurements. For this case study, the measured thermal profile was used to improve the FDM-generated profile shown in Fig. 6(c). The two-dimensional (2-D) FDM thermal profile was constructed by implementing a representative converter geometry into a spreadsheet environment,[1] as is shown in Fig. 6(a) for the conventional converter. Each spreadsheet cell has an initial temperature and by iteration calculates the change in temperature by the discrete form function for thermal conduction

$$T_x = \frac{\sum_{I=1}^{n} \frac{T_i}{R_{\theta(j-x)}} + Q_x}{\sum_{i=1}^{n} \frac{1}{R_{\theta(j-x)}}} \qquad (8)$$

where

Q_x	Δ energy in cell [W];
n	number of neighboring cells: four for 2-D analysis or six for 3-D analysis;
$R_{\theta(j-x)}$	equivalent thermal resistance [$f(\lambda, \bar{h}_c, \bar{h}_r, l)$] between neighboring cell j and cell x;
λ	thermal conductivity of the material [W/m · k];
$\bar{h}_c$	coefficient of convective heat transfer [W/m²];
$\bar{h}_r$	coefficient of radiative heat transfer [W/m² · K⁴];
l	length between neighboring cells.

The thermal profile is then used as a map to place underheated components at positions where their required temperature differences, to reach their optimal temperature, are alleviated as far as possible. By placing the underheated components close to the overheated components, the overheated components cool down while the underheated components heat up, helping each other reach their optimal temperature. Again, an FDM model is used to verify that the new component placement actually leads to a more uniform temperature profile. This is done by adjusting the representative spreadsheet geometry to resemble the new component placement. If this layout is performed correctly, one could have both over- and underheated components operating at their own optimal temperatures. A rigorous discussion on the details regarding the layout strategy lies beyond the scope of this paper. Avid readers are referred to [13] for an in-depth look on the component-layout strategy itself.

An improved component placement for the conventional converter is shown in Fig. 6(b), which leads to the thermal profile shown in Fig. 6(d). A thermal peak can still be identified. This is due to the model not incorporating the effect of thermal interface material directly between components. The effect of the thermal interface material can be seen as large when considering that the converter will be folded to allow thermal coupling between many of the components. Implementing thermal interface material between adjacent components, thermal vias, and copper planes on the PCB is one of the measures to spread the heat more equally among all components. Geometrical limitations exist, which limit the success of this method. The measured thermal profile of both the conventional converter design and the flex-solution converter is shown in Fig. 5. The performance and improvements are discussed next.

V. CONVERTER PERFORMANCE

The solution using only flex technology, shown in Fig. 3(c), has been designed based on the methods shown in Section IV. This implies placing components at exact locations where the effect of the neighboring component temperatures, together with the components' own heat generation, will allow it to operate close to the components' optimal material temperature.

---

[1] 1 spreadsheet cell = 1 mm² on converter surface.
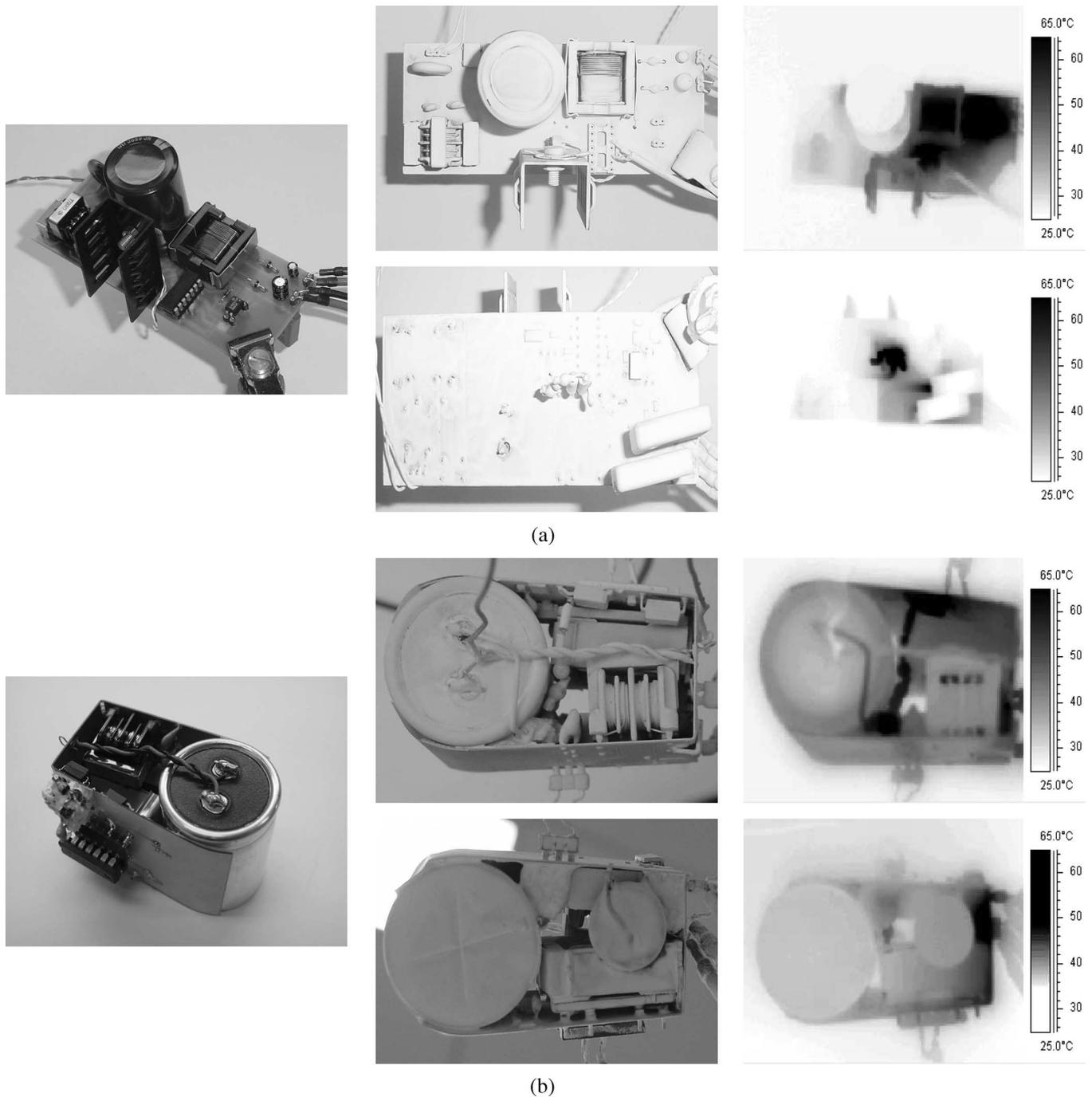
Fig. 4. Case-study converters. (left) Optical image showing individual components and (center) optical image showing components covered in white powder that corresponds with (right) thermal image showing surface temperatures. Thermal images taken at steady state under full-load conditions. Output power level during thermal measurement is indicated for each converter. (a) Conventional converter (19.8 W). (b) Flex-solution converter (21.5 W).

An example of this is the thermal connection of the input electrolytic-capacitor canister to the inductor ferrite, as well as placing the underheated line filters in close proximity of the overheated output rectifying diodes. All available possibilities for thermal coupling are also exploited, such as using thermal interface material, thermal vias, copper planes on PCB as thermal layers, and using conductive component housings as heat spreaders to realize this, as shown in Fig. 7. These exploits allow the complete removal of the MOSFET switch's heatsink, as the entire converter outer surface now contributes to thermal convection due to the good thermal interconnection between components and through thermal conduction of the PCB copper planes on which the MOSFET switch is now mounted.

Furthermore, the top and bottom of the converter are left open to take advantage of the chimney effect inside the rolled-up converter. The chimney effect is created by the components at the bottom of the converter heating up the air around it, forcing convection cooling on all the components higher up in the converter where the rising hot air passes by. This reason and the ability to use IR thermography on the open ends of the converter to facilitate thermal measurements of the enclosed components have been the decisive factor for choosing to build the

(a)

(b)
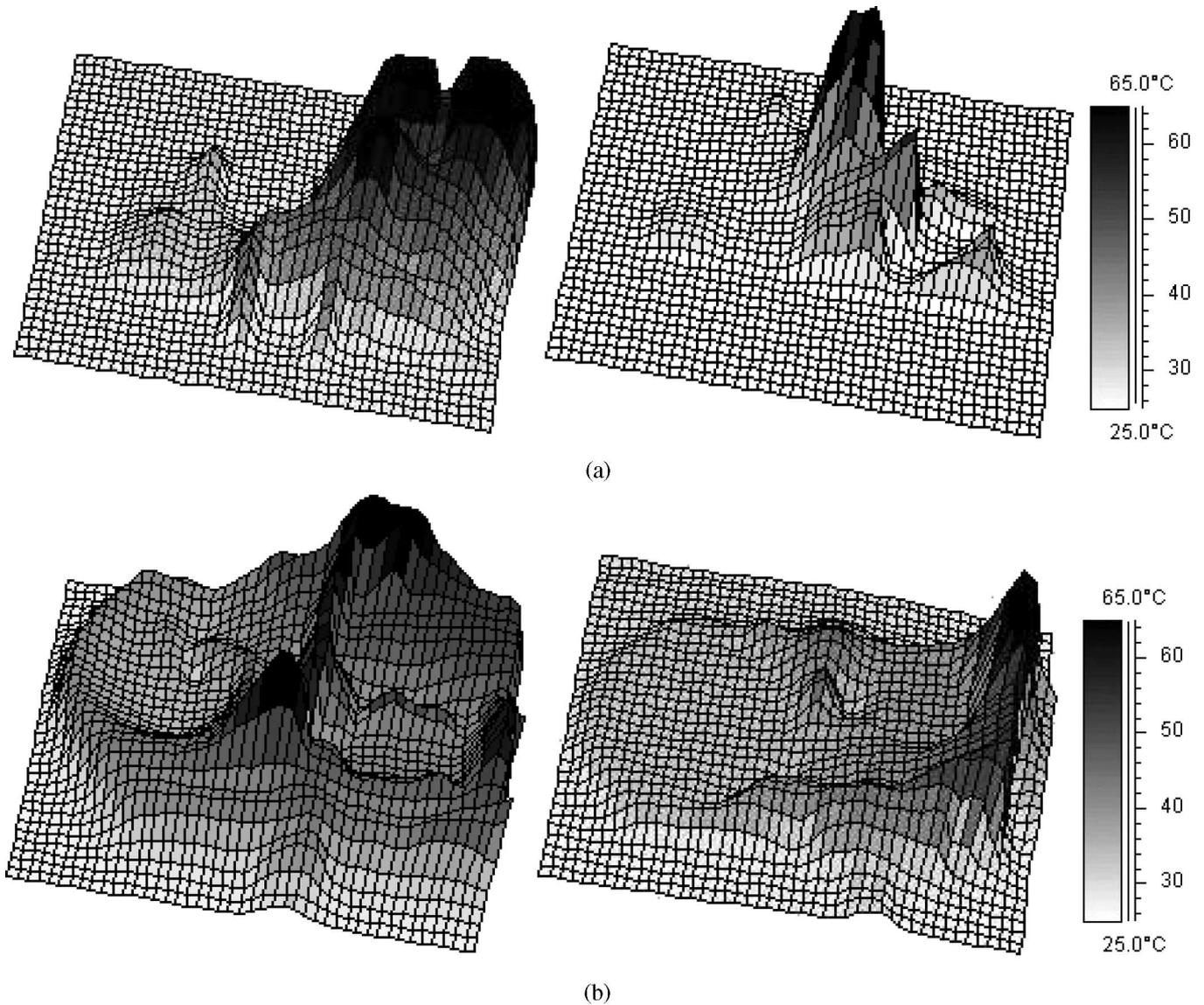
Fig. 5. Thermal profile of case-study converters viewed from (left) top and from (right) bottom using same temperature scale and converter orientation as in Fig. 4. (a) Conventional converter. (b) Flex-solution converter.

TABLE III
THERMAL MANAGEMENT—EXTRACT OF COMPONENT EVALUATION
FOR CONVENTIONAL CONVERTER DESIGN

Component	$T[^\circ C]$	Power density $TDR[\%]$	$\Delta T[^\circ C]$
Input filter C	27.5	0.27	+42.5
+12V filter C	60.0	71.47	+10.0
+5V filter C	68.8	99.53	+1.2
Snubber C	112.0	0.32	-42.0
Snubber R	112.0	99.00	-2.0
Coupled L	72.0	98.82	+3.0
Bridge Rectifier	38.0	2.4×10^{-4}	+72.0
+12V rectifying D	103.0	88.47	+7.0
+5V rectifying D	114.0	96.07	-4.0
MOSFET switch	50.0	1.2×10^{-2}	+60.0

flex solution as improved technology carrier in this case study above the hard-to-manufacture-and-measure rigid-flex solution. For prototyping, the flex material has been substituted by a very thin FR4 substrate (double sided) in the design. This limits the flexibility and mildly complicates manufacturing. For example, to facilitate bending of corners, little to no copper is allowed on the folding edge, which serves as the thermal connection between two segments of the converter. This diminishes the thermal-spreading capability of this converter in comparison with the one implementing the actual flexible PCB substrate, resulting in more difficulty to achieve a uniform surface temperature. The synthesized converter is shown in Fig. 4(b) alongside its thermal measurement at full load and steady-state operation. The thermal profile associated with the thermal measurements of the flex converter is shown in Fig. 5(b). The converter has been suspended in midair to facilitate simultaneous thermal
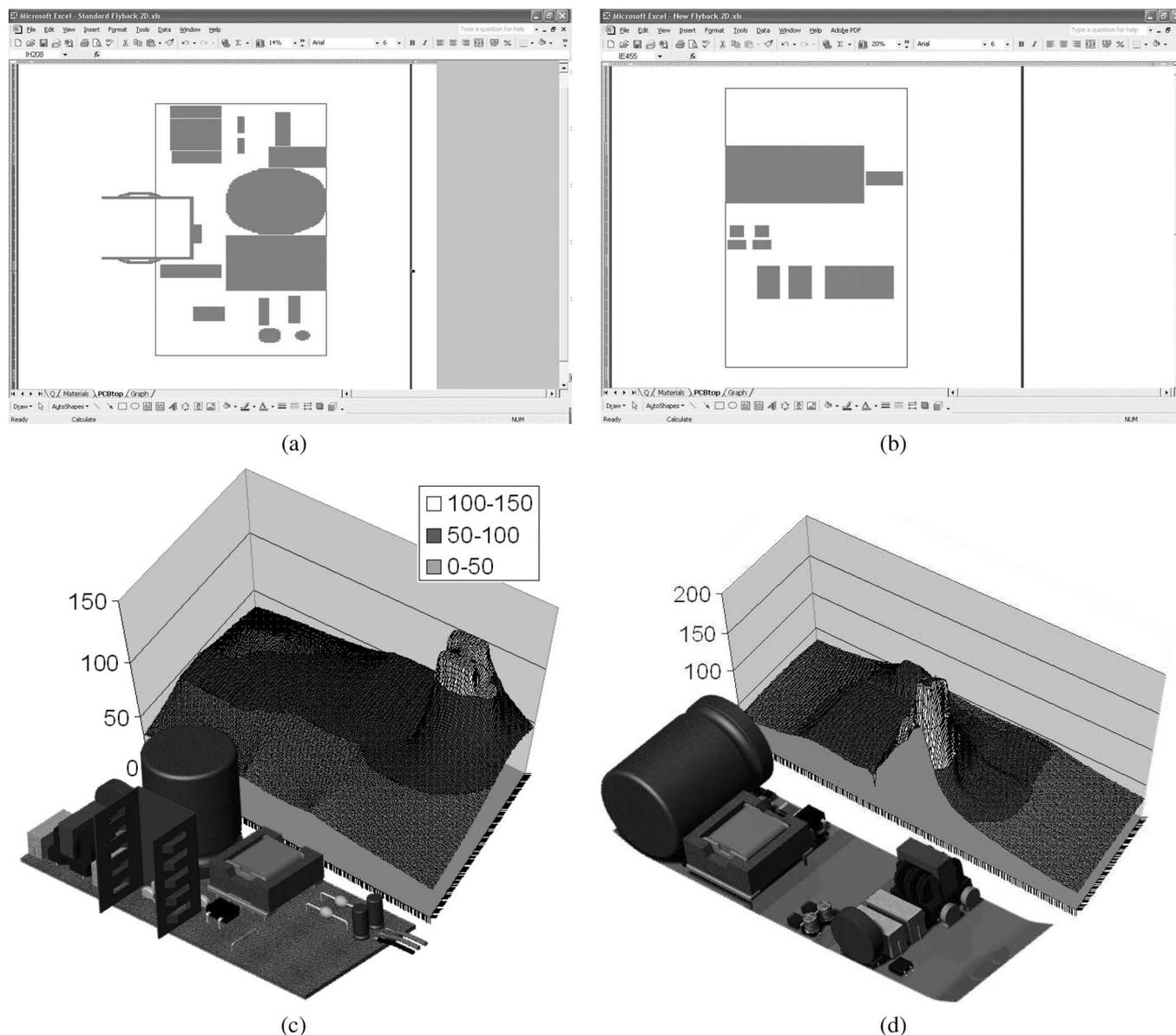
Fig. 6. FDM strategy used as tool to predict thermal improvement of component-layout concepts. (a) Representative geometry of conventional converter implemented in spreadsheet environment to predict its 2-D thermal profile. (b) Representative geometry showing component layout of proposed flex-solution converter. (c) Conventional converter layout along FDM predicted 2-D thermal profile along PCB top surface. (d) Proposed flex-solution component layout alongside 2-D FDM predicted thermal profile excluding influence of intercomponent thermal interface material.

measurement from the top as well as the bottom of the converter without changing the converter orientation and subsequent thermal system.

The converters' environments, i.e., its enclosure and intended surroundings, also play an important role in its thermal performance and also need to be addressed. The converter here is enclosed in a "virtual" cover, allowing perfect thermal transport from the outer surface to the ambient without any thermal spreading across its outer surface, i.e., air barrier. This is done to illustrate the concept clearly as well as allow for IR thermography of all the components. The concept, however, is not restricted to converters with this "virtual" enclosure and will perform equally well if a cover is used, which does alter the thermal management, as long as the cover is then also included in the thermal analysis from the start.

From the thermal measurements, the surface temperatures of the individual components can be measured, and the performance criteria are applied. Table IV shows the surface temperatures and TDR for some important components from both the conventional- and the flex-solution Flyback converter for power density and reliability objectives. From Table IV, it can be seen that the surface temperatures for the input filter capacitor, snubber capacitor, bridge rectifier, and MOSFET switch have increased, improving their figure-of-merit ratings with respect to power density accordingly. This is good because it shows that the invested material is now used more productively. The rest of the component temperatures have all decreased, resulting in lower figure-of-merit ratings for achieving high power density. At first glance, it seems that the new converter rates are poorer for high power density by the rating method
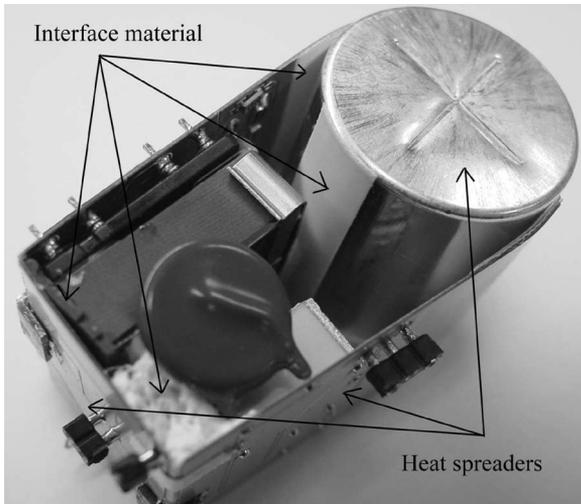
Fig. 7. Some measures taken to ensure good thermal interconnection between components in flex-solution Flyback converter. Sheet and gel-type thermal interface material connects larger assemblies; thermal vias allow for heat spreading between two PCB copper layers, which, in connection with thermally connected component surfaces, also act as heat spreaders.

applied; this is, however, not the case. By thermally coupling all the components together, multiple parallel heat flow paths are created. This reduces the effective thermal resistance between the components and the ambient. This is then responsible for reducing the number of extreme high temperatures, or so-called "hotspots," on the PCB, equalizing the thermal profile on the external surface of the converter sufficiently and, in so doing, approaching the set objective of a uniform surface-temperature profile. This is clearly visible in the more uniform temperature profile of the flex-converter design [shown in Fig. 5(b)] in comparison with the conventional design shown in Fig. 5(a). The extent in which this heat sharing takes place in the flex converter, however, brings the operating temperatures down so far that the rating system indicates that the invested material is now underutilized even more. This actually means that there is now an increased margin created for every component to reduce the material and packaging further and increase the power density in that way. By tighter layout or removing even more unused packaging material of components, or alternatively by increasing the rated power level of the converter as it is, the created margin can be utilized effectively to reach high power densities. The figure-of-merit ratings for exactly the same converter measurement, but calculated from a reliability objective, have increased for all components, as shown in the reliability column of Table IV. This shows that all components are operating closer to their optimal temperature as set for reliability. If the power level of this converter is increased to achieve high power density, the reliability of the components will have to pay the price. The figure-of-merit system quantifies this very well. One could classify the flex-solution converter as a more reliable converter with increased potential for high power density.

Table V shows the figures of merit for the conventional converter design and the geometrically integrated solutions proposed in Section III. Table V shows the TMLD for two scenarios: one where the enclosed air in the converter is included

in the calculation (air) and one where it is neglected (no air). From the TMLD value where air is included, one can compare the thermal-management effectiveness based on the density of the thermal losses transported by the converter material including the air as thermal-transport medium. The conventional thermal management exhibits an $\approx 96\ \mu\text{W/mm}^3$ thermal-loss density in its thermal-conducting material, whereas the flex solution exhibits a density of more than eight times this value $\approx 814\ \mu\text{W/mm}^3$. This indicates a much more intensified use of the invested material in the flex-converter thermal design and can be traced back in the power densities achieved of twice that of the conventional design. The same comparison can be performed for the TMLD value, which does not include the enclosed air. Here, the values are considerably higher due to the restrictive air barrier in the converter not playing a role in the thermal management. Furthermore, the same incremental trend can be observed except for the rigid-flex solution, which has a relatively low value. This indicates that too much dedicated thermal-conducting material has been invested in this design. It will therefore be a relatively expensive solution to build in comparison to the conventional and flex solutions. Think of the cost of additional, or thicker, copper layers, which prove to be overdesigned for this converters' dissipation level. Reducing the thickness or the amount of copper layers in the rigid PCB segments will already help reduce these costs, keeping in mind that copper is a relatively expensive commodity. The improvement will then be indicated by higher TMLD values. For example, just by reducing the main thermal-layer thickness from 350 to 150 μm, an increase from ≈ 409 to $\approx 730\ \mu\text{W/mm}^3$ (78% increase) is achieved in TMLD value for the rigid-flex solution. The flex solution uses very thin copper layers to maintain its flexibility, and therefore, a high thermal-loss density is achieved, and likewise, a high TMLD value of $\approx 17\ \text{mW/mm}^3$. The TDR values for the overall converter were calculated using a weighted sum (ws) method with all weights being equal to one, i.e., $a_1 = a_2 = \cdots = a_n = 1$ and, second, by setting an optimal band at 1%, 50%, and 85% of the theoretical optimum of the overall converter ($\alpha = 0.01; 0.5; 0.85$), respectively. When comparing the TDRs for the overall converters based on power-density objective, the ratings show that the thermal management of the flex converter has improved to such an extent that 53.1% of the components now operates in the set optimal thermal band of 1% instead of the 29% of the components in the conventional converter. Zero percentage of the components operate in the set optimal bands of 50% and 85%. This shows the huge margin of improvement that still exists for this converter. The TDRs for reliability gives a whole different perspective on the flex converter. Almost all components operate in an optimal band of 50%, and as much as 46.9% operate in the optimal band of 85% in comparison with nearly half the components of the conventional design operating in the 50% optimal band and only 3.2% operating in the 85% optimal band. This shows that the thermal-management technique succeeded in realizing a more reliable converter solution on a component level, which has improved power density and potential for even higher power densities. The achieved power densities shown in Table V illustrate what combined geometric and thermal integration can achieve but is far lower than what

TABLE IV
FIGURE-OF-MERIT COMPARISON FOR EXTRACT OF COMPONENTS FROM CONVENTIONAL AND IMPROVED CONVERTER DESIGNS

Component	Conventional			Flex		
	$T[^\circ C]$	Power density $TDR[\%]$	Reliability $TDR[\%]$	$T[^\circ C]$	Power density $TDR[\%]$	Reliability $TDR[\%]$
Input filter C	27.5	0.27	51.20	40.3	5.61	88.30
+12V filter C	60.0	71.47	87.62	53.0	38.92	98.82
+5V filter C	68.8	99.53	62.67	53.8	42.45	98.10
Snubber C	112.0	0.32	0.62	60.3	73.55	86.91
Snubber R	112.0	99.00	37.78	70.6	2.06	98.63
Coupled L	72.0	98.82	81.42	51.4	47.88	99.08
Bridge Rectifier	38.0	2.4×10^{-4}	37.78	49.0	9.1×10^{-3}	61.83
+12V rectifying D	103.0	88.47	57.26	80.0	10.54	97.95
+5V rectifying D	114.0	96.07	33.90	80.4	11.19	98.24
MOSFET switch	50.0	0.01	64.12	76.8	6.35	99.77

TABLE V
THERMAL-MANAGEMENT EVALUATION—FIGURES OF MERIT OF CONVENTIONAL AND IMPROVED CONVERTER DESIGNS

		Conventional	Rigid-Flex	Flex
TMLD	Air	95.85	114.36	813.89
$\left[\frac{\mu W}{mm^3}\right]$	No air	2226.52	409.34	17092.32
TDR (Power density)	$ws(a=1)$	18.5	n/a	11.4
[%]	$\alpha = 0.01$	29.0	n/a	53.1
(Reliability)	$ws(a=1)$	49.3	n/a	80.2
TDR	$\alpha = 0.01$	96.8	n/a	100.0
[%]	$\alpha = 0.5$	48.4	n/a	96.9
	$\alpha = 0.85$	3.2	n/a	46.9
Power density $[W/l]$		150	250	300

is possible if the thermal margin established by the thermal integration performed in the flex solution is fully exploited.

1) Future Advances Using Integration Technologies: The integration technologies used in this publication were limited to geometrical integration of the bulky components identified in a typical ac–dc converter and the thermal integration thereof [compare Figs. 3(a) and 4(a) with Figs. 3(c) and 4(b)]. This could be expanded to also include electromagnetic integration of passives into the PCB itself as further advancement of the integration technology, as conceptually proposed in Fig. 3(b). EmPIC technology [6], [14]–[16] can be combined with low-profile inductor integration processes currently under investigation by Ludwig *et al.* [17] to realize this type of integration. Implementing square bus capacitors, available from EPCOS, instead of the round electrolytic capacitor used here could also ease the geometrical integration. By means of the figure-of-merit system, which is derived and used here, all three integration technologies can be optimized individually and also collectively in a minimum amount of iterations to achieve high power densities in PCB assembled switch mode converters.

VI. CONCLUSION

This paper presents design techniques for switch mode converters where the focus lies strongly on the thermal design, or, more specifically, the thermal management of the converter itself. Integration technologies contribute to higher achievable power densities and reduced average PCB temperatures. Key features include optimized heat spreading on the enclosure to optimize convection to the ambient as well as optimized thermal paths for individual components. The figure-of-merit theory necessary to critically compare thermal-management effectiveness and overall thermal design, developed in this paper, aids in judging improvement objectively and pinpoints where room still exists for improvement in a quantitative manner. Power density as well as reliability criteria was considered during the investigation and was critically compared. FDM analysis has been shown to aid in 3-D thermal design by creating a thermal map for components to be relocated based on their thermal-management figure-of-merit requirements. Experiments validate the proposed improvements that have been identified by means of the proposed figure-of-merit guided design approach. Possibilities to further improve on thermal management of ac–dc converters using integration technologies have been identified.

REFERENCES

[1] N. Hallwood, "Effective thermal design and management," in *Proc. IEE Colloq. Comput. Aided Design Tools for Thermal Manage.*, Dec. 1989, pp. 5/1–5/3.

[2] S. Jones, D. Pye, and T. Jeal, "Modern materials technologies in PCB thermal management," in *Proc. IEE Colloq. CAD Tools for Thermal Manage. (Dig. 027)*, Feb. 1993, pp. 8/1–8/9.

[3] S. Tang, S. Hui, and H.-H. Chung, "A low-profile power converter using printed-circuit board (PCB) power transformer with ferrite polymer composite," *IEEE Trans. Power Electron.*, vol. 16, no. 4, pp. 493–498, Jul. 2001.

[4] S. Ben-Yaakov, *The Benefits of Planar Magnetics in HF Power Conversion*, 2001. [Online]. Available: http://www.paytongroup.com

[5] J. Strydom, J. Ferreira, J. van Wyk, I. Hofsajer, and E. Waffenschmidt, "Power electronic subassemblies with increased functionality based on planar sub-components," in *Proc. IEEE Power Electron. Spec. Conf.*, Jun. 2000, vol. 3, pp. 1273–1278.

[6] E. Waffenschmidt and J. Ferreira, "Embedded passives integrated circuits for power converters," in *Proc. IEEE Power Electron. Spec. Conf.*, Jun. 2002, vol. 1, pp. 12–17.

[7] D. Grafham, (2004). Optimal thermal management of planar magnetics in high frequency SMPS. Application note-001. [Online]. Available: http://www.paytongroup.com/Catalogue/cat_p26.pdf

[8] J. Ferreira, I. Hofsajer, and J. van Wyk, "Exploiting the third dimension in power electronics packaging," in *Proc. IEEE Appl. Power Electron. Conf. and Expo.*, Feb. 1997, vol. 1, pp. 419–423.

[9] A. Lostetter, F. Barlow, A. Elshabini, K. Olejniczak, and S. Ang, "Polymer Thick Film (PTF) and flex technologies for low cost power electronics packaging," in *Proc. IWIPP*, Jul. 2000, vol. 1, pp. 33–40.

[10] I. Hofsajer, J. Ferreira, and J. van Wyk, "A new manufacturing and packaging technology for the integration of power electronics," in *Proc. IEEE Ind. Appl. Conf.*, Oct. 1995, vol. 1, pp. 891–897.

[11] E. de Jong, J. Ferreira, and P. Bauer, "Evaluating thermal management efficiency in converters," in *Proc. IEEE Power Electron. Spec. Conf.*, Jun. 2004, pp. 4881–4887.

[12] ——, "Improving the thermal management of ac–dc converters using integration technologies," in *Proc. IEEE Ind. Appl. Conf.*, Oct. 2004, vol. 4, pp. 2315–2322.

[13] ——, "Thermal model extraction as means to thermal management improvement in PCB assembled power converters," in *Proc. PCIM Conf.*, Jun. 2005, vol. 1, pp. 240–245.

[14] E. Waffenschmidt, "A transformer with integrated capacitor in a crosswise connected configuration: Measurements and calculations of its behavior," in *Proc. IEEE 31st Annu. PESC*, Jun. 2000, vol. 3, pp. 1627–1632.

[15] J. Ferreira, E. Waffenschmidt, J. Strydom, and J. van Wyk, "Embedded capacitance in the PCB of switchmode converters," in *Proc. IEEE Power Electron. Spec. Conf.*, Jun. 2002, vol. 1, pp. 119–123.

[16] J. Ferreira and E. Waffenschmidt, "Low profile switchmode converter with embedded passive components in the PCB," *EPE J.*, vol. 13, no. 2, pp. 11–20, May 2003.

[17] M. Ludwig, M. Duffy, T. O'Donnel, P. McCloskey, and S. O. Matuna, "Design study for ultraflat PCB-integrated inductors for low-power conversion applications," *IEEE Trans. Magn.*, vol. 39, no. 5, pp. 3193–3195, Sep. 2003.

J. A. Ferreira (M'88–SM'01–F'05) received the B.Sc.Eng., M.Sc.Eng., and Ph.D. degrees in electrical engineering from the Rand Afrikaans University, Johannesburg, South Africa, in 1981, 1983, and 1988, respectively.

In 1981, he was with the Institute of Power Electronics and Electric Drives, Technical University of Aachen, and worked in industry at ESD (Pty) Ltd., from 1982 to 1985. From 1986 to 1997, he was with the Faculty of Engineering, Rand Afrikaans University, where he held the Carl and Emily Fuchs Chair of Power Electronics in later years. Since 1998, he has been a Professor with the Delft University of Technology, Delft, The Netherlands.

Dr. Ferreira was Chairman of the South African Section of the IEEE, from 1993 to 1994. He is the Founding Chairman of the IEEE Joint IndustryApplications Society/Power Electronics Society (IAS/PELS) Benelux Chapter. He served as the Transactions Review Chairman of the IEEE IAS Power-Electronic Devices and Components committee and is an Associate Editor of the PELS Transactions. He was a member of the IEEE Power Electronics Specialists Conference (PESC) Adcom. He is currently the Treasurer of the IEEE PELS. He served as Chairman of the CIGRE SC14 National Committee of the Netherlands and was a member of the executive committee of the European Power Electronics and Drives Association (EPE) Society.

Erik C. W. de Jong (S'06) was born in Johannesburg, South Africa. He received the B.Ing. (*cum laude*) and M.Ing. (*cum laude*) degrees in electric and electronic engineering from the Rand Afrikaans University, Johannesburg, in 2001 and 2003, respectively. He is currently working toward the Ph.D. degree in electromagnetic integration technology and thermal management in PCB power supplies at Delft University of Technology, Delft, The Netherlands.

His fields of interest include high-frequency dc–dc converters and integration technologies in printed-circuit boards. He is currently with the Electrical Power Processing group at the EWI faculty of the Delft University of Technology.

Pavol Bauer (S'91–M'00) received the M.S. degree in electrical engineering from the Technical University of Kosice, Kosice, Slovakia, in 1985, and the Ph.D. degree from Delft University of Technology, Delft, The Netherlands, in 1994.

Since 1990, he has been with the Delft University of Technology, teaching power electronics, electrical drives, and related subjects. He has published over 150 papers in this field. He holds an international patent and has organized several tutorials.